Protein Expression and Purification 151 (2018) 23–29

Contents lists available at ScienceDirect

Protein Expression and Purification

journal homepage: www.elsevier.com/locate/yprep

Increased soluble heterologous expression of a rat brain 3-*O*-sulfotransferase 1 – A key enzyme for heparin biosynthesis

Weihua Jin[a], Shuai Li[a], Jiale Chen[a], Bing Liu[a], Jie Li[a], Xueliang Li[a], Fuming Zhang[b], Robert J. Linhardt[b,c], Weihong Zhong[a,*]

[a] College of Biotechnology and Bioengineering, Zhejiang University of Technology, Hangzhou, 310032, China
[b] Department of Chemical and Biological Engineering, Center for Biotechnology and Interdisciplinary Studies, Rensselaer Polytechnic Institute, Troy, NY, 12180, USA
[c] Department of Biological Science, Departments of Chemistry and Chemical Biology and Biomedical Engineering, Center for Biotechnology and Interdisciplinary Studies, Rensselaer Polytechnic Institute, Troy, NY, 12180, USA

ARTICLE INFO

Keywords:
Heparan sulfate
3-*O*-sulfotransferases
Heterologous expression
Rat brain
Codon optimization

ABSTRACT

Heparan sulfate (HS), is a glycosaminoglycan (GAG) involved in various biological processes, including blood coagulation, wound healing and embryonic development. HS 3-*O*-sulfotransferases (3-OST), which transfer the sulfo group to the 3-hydroxyl group of certain glucosamine residues, is a key enzyme in the biosynthesis of a number of biologically important HS chains. The 3-OST-1 isoform is one of the 7 known 3-OST isoforms and is important for the biosynthesis of anticoagulant HS chains. In this study, we cloned 3-OST-1 from the rat brain by reverse transcription-polymerase chain reaction (RT-PCR). After codon optimization and removal of the signal peptide, the recombinant plasmid was transformed into *Escherichia coli* BL21 (DE3) to obtain a His tagged-3-OST-1 fusion protein. SDS-PAGE analysis showed that the expressed 3-OST-1 was mainly found in inclusion bodies. The 3-OST-1 was purified by Ni affinity column and refolded by dialysis. The activity of obtained 3-OST-1 was 0.04 U/mL with a specific activity of 0.55 U/mg after renaturation. Furthermore, a co-expressed recombinant plasmid pET-28a-3-OST-1 with the chaperone expression system (pGro7) was constructed and transferred to *E. coli* BL21 (DE3) to co-express recombinant strain *E. coli* BL21 (DE3)/pET-28a-3-OST-1 + pGro7. The soluble expression of 3-OST-1 was significantly improved in the co-expressed recombinant strain, with enzyme activity reaching 0.06 U/mL and having a specific activity of 0.83 U/mg. *N*-sulfo, *N*-acetylheparosan (NSNAH) was modified by the recombinant expressed 3-OST-1 and the product was confirmed by ^{1}H NMR showing the sulfo group was successfully transferred to NSNAH.

1. Introduction

Heparan sulfate (HS) plays a key role in a variety of important biological processes including virus infection, regulation of blood coagulation, embryonic development, inflammation, tumor growth inhibition [1–5]. HS and heparin is made up of repeating disaccharide units of consisting of glucosamine and glucuronic acid residues. In biosynthesis, heparosan is formed by alternately adding glucosamine and glucuronic acid to the non-reducing end of the chain [6]. Subsequently, this high-molecular heparosan is modified by a series of enzymatic reactions, including *N*-deacetylation, *N*-sulfation [7], glucuronic acid C5 epimerization, and *O*-sulfation at different positions and to different levels [8]. Due to the incompleteness of these modifications, the synthesized HS polysaccharides also have different structures. The interactions of HS with different proteins depend on the sites and *O*-sulfation levels of the polysaccharide chains [9]. In recent years, many studies have shown that HS and its derivatives play important roles in virus infection [10,11]. A HS chain containing a 3-*O*-sulfo-D-glucosamine residue was found to bind to viral glycoprotein D protein and block the interaction between HSV-1 virus and cell surface proteoglycans [12]. In addition, 3-*O*-sulfo group containing HS chain can bind to antithrombin III, HSV-1 glycoprotein D, fibroblast growth factor/receptor (FGF/FGFR) [13,14] and has a role in ovulation [15].

HS 3-*O*-sulfotransferases (3-OST) catalyzes the transfer of sulfo groups to the 3-hydroxyl group of certain glucosamine residues. The 3-OST gene has been cloned from endothelial cells of newborn mice and human umbilical vein endothelial cells, and the 3-OST enzyme was heterologously expressed [16]. The structure of HS is altered spatiotemporally for regulating plenty of biological activities in the developing brain including the proliferation of neuronal progenitors, extension of axons and formation of dendrites [17]. These sulfotransferases including 3-OST were important in the signaling of several HS-binding

* Corresponding author.
E-mail address: whzhong@zjut.edu.cn (W. Zhong).

https://doi.org/10.1016/j.pep.2018.06.007
Received 9 May 2018; Received in revised form 8 June 2018; Accepted 8 June 2018
Available online 09 June 2018
1046-5928/

proteins in the mouse brain [17]. There is no report on the heterologously expression of 3-OST gene from cells of rat brain. Although the genome of mice is more closely related to human genome than rat's, research on heterologous expression of 3-OST gene from rat brain cell would enrich the knowledge on structure and functions of sulfotransferases from diverse source. Additionally, the 3-OST from rat brain cell may supply one more potential selection to be a tool enzyme for heparin preparation from heparosan. Among the 7 isoforms of 3-OST [18], 3-OST-1 is the rate-limiting enzyme, controlling cellular production of the critical active structure [19]. Therefore, 3-OST-1 was selected for cloning and expressing in *E. coli* in our current study. Codon optimization was performed for the 3-OST-1 gene and the signal peptide was removed to achieve efficient heterologous expression of the target protein. Codon selection and distribution is one of the factors that affect the efficient heterologously expression of genes. Optimizing the codon sequence on exogenous genes could improve heterologous protein expression. While signal peptides of eukaryotes are expressed in prokaryotes, most of these do not have secretive function, and are always fused with the target protein, affecting the correct folding and function of the target protein [20].

In this paper, to achieve effectively heterologous expression of the exogenous protein in *E. coli*, the 3-OST-1 gene was inserted into the His-tagged pET-28a expression plasmid, which contains a strong promoter of T7 Lac capable of rapidly and stably transcribing downstream genes under the action of the host bacterial with T7 RNA polymerase. At the same time, the His-tag carried by the vector helps purify the His-tag fused target protein. Finally, the enzyme activity, of the protein obtained, was measured using a 3′-phosphoadenosine-5′-phosphosulfate (PAPS) regeneration system [21]. ^{1}H NMR spectrum was conducted to confirm that 3-OST-1 could successfully transfer a sulfo group to the specific site of the substrate *N*-sulfo, *N*-acetylheparosan (NSNAH).

2. Materials and methods

2.1. Animals, strains, plasmids, enzymes and reagents

The Wistar Rats were purchased from the China National Laboratory Animal Resource Center (Shanghai, China).

The *E. coli* DH5α, *E. coli* TransB (DE3) and *E. coli* BL21 (DE3) were purchased from TransGen Biotech. The pMD-19-T vector and pMAL-c2X were obtained from TAKARA and Beijing Dingguo Biotechnology (China), respectively. The plasmid pET-28a and pet 20 b were obtained from Sangon Biotech (Shanghai, China) and the plasmid pGro7 was obtained from TAKARA.

The reagents for PCR were purchased from Sigma (St. Louis, MO). The oligonucleotide primers were synthesized from Sangon Biotech (Shanghai, China). Ni-NTA Sefinose™ Resin Kit was purchased from Sangon Biotech. The NSNAH were prepared in our laboratory.

2.2. RT-PCR

The HS3-OST-1 sequence was obtained from Genebank (the accession number was **NM_053391.1**). Based on the sequence, two specific primers, which contained *Bam* H I and *Hin* d III restriction enzyme sites, were synthesized. The total RNA of the Wistar rat brain was extracted, and cDNA was synthetized as described previously. 3-OST-1 from the Wistar rat brain was cloned by RT-PCR.

The PCR products were connected to the pMD-19-T vector. *E. coli* DH5α was used for the propagation of recombinant plasmids. The competent DH5α cells were transformed with cloning vector pMD-19-T by white and blue screening. Recombinants were sequenced by Introversion (Shanghai) to verify the correct nucleotide sequencing.

2.3. Codon optimization

After sequencing, the rare codons of the sequence were analyzed and the codons were optimized by Synbio Technology (Suzhou).

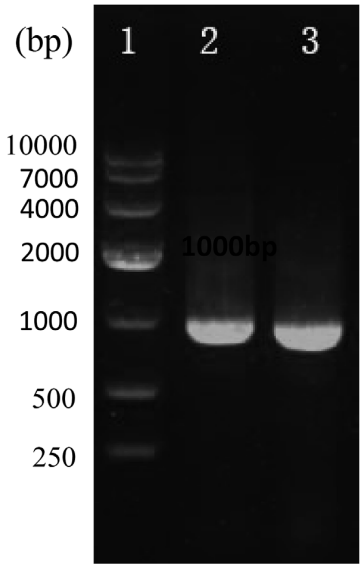

Fig. 1. PCR product of rat 3-OST-1. Lane 1, DNA marker; Lane 2 and 3, PCR fragment.

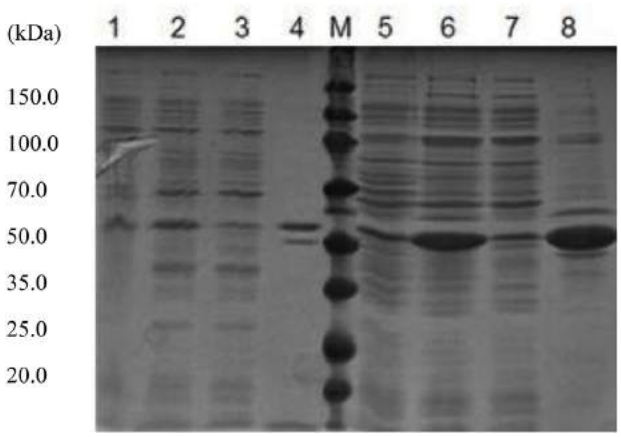

Fig. 2. Expression of 3-OST-1 via *E. coli* TransB (DE3)/pET-20b-3-OST-1 (Lane 1-4) and *E. coli* BL21 (DE3)/pET-28a-3-OST-1 (Lane 5–8). M: Protein markers; Lane 1 and 5: Un-induced total cell protein; Lane 2 and 6:Total cell protein induced by 1 mM IPTG; Lane 3 and 7: Supernatant induced by 1 mM IPTG; Lane 4 and 8: Precipitate induced by 1 mM IPTG.

2.4. Expression of 3-OST-1 gene

The gene with optimized codons was inserted into the pET-28a vector. The recombinant vector was transferred into *E. coli* BL21 (DE3) using heat transfer method. The transformant colony, *E. coli* BL21 (DE3)/pET-28a-3-OST-1, was screened on medium containing 50 mg/L kanamycin. The transformant was inoculated into 50 mL LB medium containing 50 mg/L kanamycin and incubated at 37 °C and 180 rpm. After overnight culture, the broth was inoculated into fresh LB medium containing 50 mg/L kanamycin. When the OD_{600} of the broth reached 0.6, 1 mM IPTG was added to induce the express of 3-OST-1 by the recombinant strain cultured at 22 °C and 180 rpm.

The induced host cells were harvested by centrifugation at 8000 rpm for 20 min at 4 °C. After washing, binding buffer (25 mM Tris-base, 500 mM NaCl and 10 mM imidazole, pH 8.0) was used to suspend

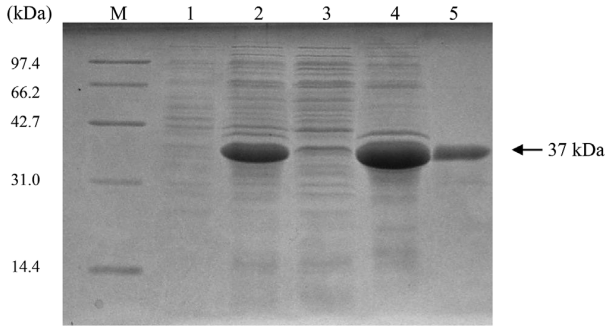

Fig. 3. Renaturation of 3-OST-1 expressed in *E. coli* BL21 (DE3)/pET-28a-3-OST-1. M: markers; Lane 1: Non-induced total cell protein; Lane 2: Total cell protein after induced by 1 mM IPTG; Lane 3: Supernatant protein after induced by 1 mM IPTG; Lane 4: Precipitate after induced by 1 mM IPTG; Lane 5: Precipitate after induced by 1 mM IPTG and using renaturation.

the bacterial cells. The suspensions were transferred to 25 mL beaker within an ultrasonic cell disintegrator (VCX500, Sonics & Materials, Inc., USA) operated at 500 W (3 s interval time, 3 s ultrasonic time) for a total of 3 min. All suspensions were kept in an ice bath during the ultrasonic process to prevent heating. SDS-PAGE was used to identify the target protein with the fragmentized liquid as total proteins, the supernatant as soluble proteins and sediment as insoluble proteins.

2.5. Protein renaturation

Dialysis was used for the renaturation. The dialysate was initially modified with 6 M urea, and then 1.5 L of renaturation solution (25 mM Tris-base, 500 mM NaCl and 10 mM imidazole, pH 8.0) was added at a rate of 0.8 mL/min to reduce the urea content in the dialysate.

2.6. Determination of enzymatic activity

At the end of refolding, the soluble recombinant protein was in the supernatant. The His-tagged 3-OST-1 was purified by Ni column with Tris-HCl buffer (pH 8.0, containing 10 mM imidazole) as binding buffer and Tris-HCl buffer (pH 8.0, containing 250 mM imidazole) as elution buffer. The elution buffer was collected and the activity of the soluble 3-OST-was determined.

Enzyme activity was determined by the *p*-nitrophenol (PNP) concentration change in a PAPS regeneration system using photometric absorbance measurements at 400 nm, which is the maximum of the absorbance peak for PNP [22]. In the PAPS regeneration system, the soluble 3-OST-1 incubated at 37 °C with NSNAH, *p*-nitrophenylsulfate (PNPS), arylsulfotransferase IV (AST-IV), and 3′-phosphoadenosine 5′-phosphate (PAP) to transfer the sulfo group from PNPS to NSNAH, resulting in the PNP production. The enzyme activity of 3-OST-1 was defined as the amount of enzyme required to catalyze the formation of 1 μmol PNP in the condition of 1 min at 37 °C and pH 7.

2.7. Sulfation of NSNAH using recombinant 3-OST-1

The experimental group contained 20 mg NSNAH, 8 mL PNPS (10 mM), 5 mL AST-IV (1 mg/mL), and 5 mL 3-OST-1 enzyme solution. The control group was the same as the experimental group but contained no NSNAH. Both groups were incubated in 37 °C for 5 min before 2 mL PAP (300 μM) was added. Then, OD_{400} value of two groups was determined in every 10 min, until OD_{400} value would not change. All samples were boiled for 5 min to stop reaction, and then filtered to remove precipitated proteins. After dialysis, concentration, and freeze-drying, the product 3-sulfo, *N*-sulfo, *N*-acetylheparosan (NSNA3SHp) was obtained.

2.8. NMR spectroscopy of NSNA3SHp

Polysaccharide (20 mg) was co-evaporated with deuterium oxide (99.9%) twice before dissolving in 0.5 mL deuterium oxide (99.9%). NMR spectrum was recorded at a Bruker AVANCE III 600 MHz at 25 °C. The spectral width was 8012.8 Hz. The relaxation delay was 1 s. The pulse angle was 45°. The acquisition time was 2.045 s. The number of scans was 32.

3. Results

3.1. 3-OST-1 gene clone and codon optimization for expression in E. coli

The total RNA was extracted from the brain of Wistar rats, and the concentration of RNA was determined using a BioTeke ND5000 ultraviolet spectrophotometer. The concentration of RNA was 369.6 ng/μL and its OD_{260}/OD_{280} was about 1.93. The resulting RNA was subjected to RT-PCR. The length of 3-OST-1 gene by PCR is same as that of *Rattus norvegicus* (936 bp) reported in NCBI (Fig. 1). The PCR products were sequenced by Qingke biological technology limited company

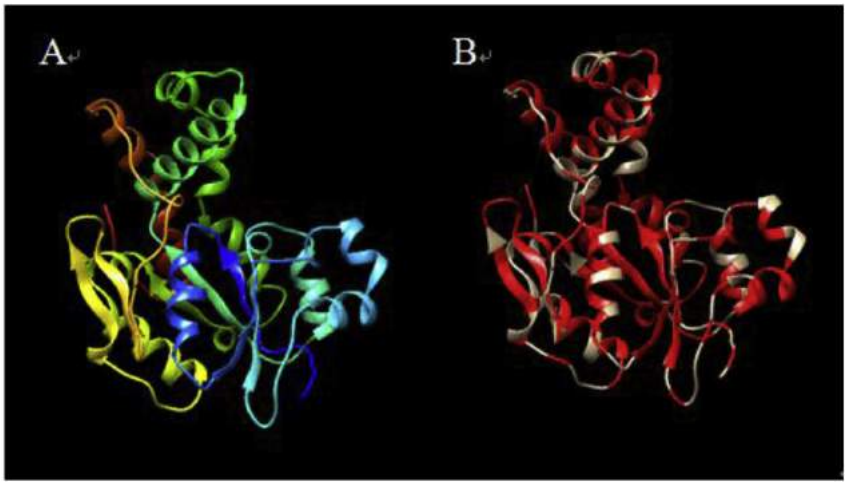

Fig. 4. 3D structure modeling (A) and hydrophobic amino acids distribution (B, Red) of 3-OST-1. (For interpretation of the references to colour in this figure legend, the reader is referred to the Web version of this article.)

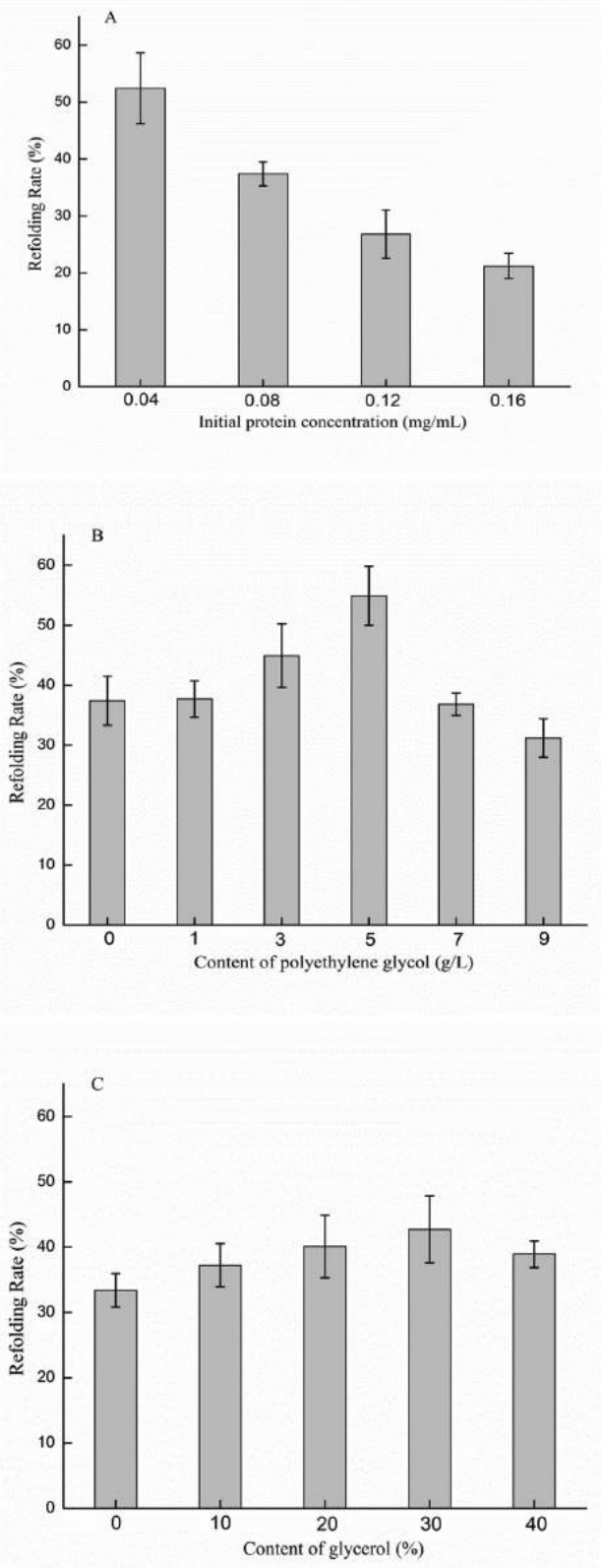

Fig. 5. Effect of initial protein concentration (A), glycerol (B), and polyethylene glycol (C) on refolding rate of 3-OST-1.

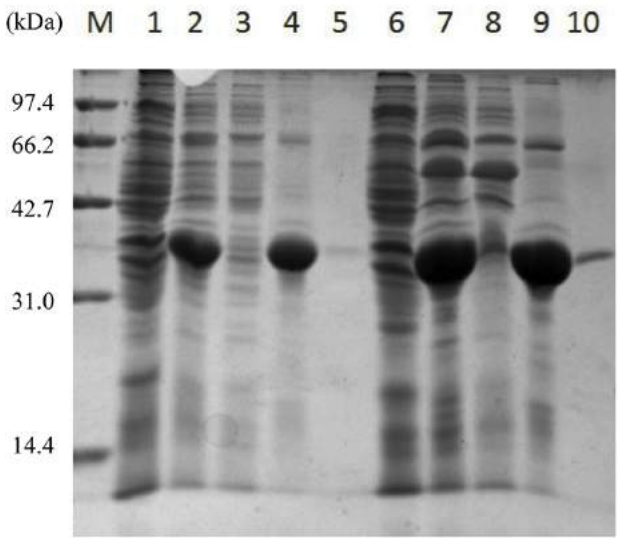

Fig. 6. Expression of 3-OST-1 by E. *coli* BL21 (DE3)/pET-28a-3-OST-1 (Lane 1–5) and *E. coli* BL21 (DE3)/pET-28a-3-OST-1 + pGro7 (Lane 6–10). M: Protein Markers; Lane 1, 6: Non-induced total cell protein; Lane 2, 7: Total cell protein after induced by 1 mM IPTG; Lane 3, 8: Supernatant after induced by 1 mM IPTG; Lane 4, 9: Cell precipitate after induced by 1 mM IPTG; Lane 5, 10: After purified by Ni-NTA column of 3, 8.

Table 1
Purification for 3-OST-1 target protein.

Strains/plasmid	Enzyme sample	Protein concentration (mg/L)	3-OST-1 concentration (U/mL)	3-OST-1 Specific activity (U/mg)
E. coli BL21 (DE3)/pET-28a-3-OST-1	Crude	620	0.03	0.05
	Ni-NTA purified	36	0.01	0.28
E. coli BL21 (DE3)/pET-28a-3-OST-1 + pGro7	Crude	911	0.04	0.04
	Ni-NTA purified	69	0.06	0.87

(Hangzhou, China) and analyzed by DNAMAN software. The gene sequences of 3-OST-1 were compared to that of *Rattus norvegicus* (GenBank accession number: NO. NM 053391.1), shown in Fig. S1, and indicated 99% homology with 5 base differences. Furthermore, a total of 15 rare codons were found in the 936 nucleotides of 3-OST-1 gene. The codons of 3-OST-1 gene required optimization to eliminate the influence of the rare codon on the expression in *E. coli*. The eukaryotic signal peptide, the sequence of signal peptide in 3-OST-1 was not suitable for secretion from prokaryotic cells and could result in reduced activity, so it was deleted. Codon optimization and signal peptide sequence deletion of 3-OST-1 were carried out by Synbio Technology (Nanjing, China). The final optimized sequence is shown in Fig. S2 and submitted to Genbank with an accession number (**MH137253**).

3.2. The expression of 3-OST-1 gene in E. coli BL21 (DE3)/pET-28a-3-OST-1 and E. coli TransB (DE3)/pET-20b-3-OST-1

The recombinant plasmid with the optimized target fragment pET-28a-3-OST- 1 was transformed into *E. coli* BL21 (DE3) to express the target protein. The final recombinant strain *E. coli* BL21 (DE3)/pET-28a-3-OST-1 could express 3-OST-1 after IPTG induction, as confirmed by SDS-PAGE (Fig. 2, Lane 5–8). The yield of 3-OST-1 significantly increased after IPTG induction (Lane 6 and 8).

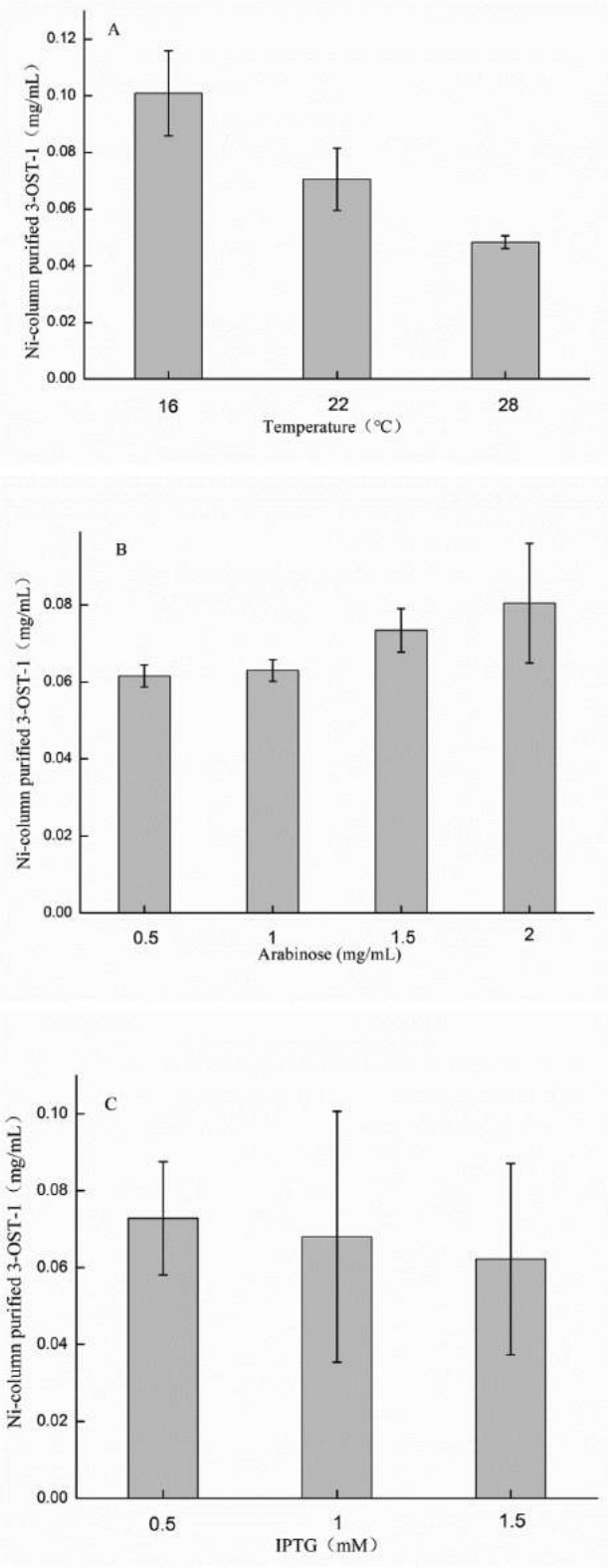

Fig. 7. Effect of inducing temperature (A), Arabinose (B), and IPTG (C) concentration on the expression of *E. coli* BL21 (DE3)/pET-28a-3-OST-1 + pGro7 induced purified by Ni-NTA column.

Meanwhile, the optimized target fragment was also inserted into the pET-20 b plasmid, which had a signal peptide sequence to construct a recombinant plasmid pET-20b-3-OST-1. After transferring the plasmid into the host cells, a recombinant strain *E. coli* TransB (DE3)/pET-20b-3-OST-1 was successfully constructed. The expression of 3-OST-1 after IPTG induction was also detected (Fig. 2, Lane 2 and 4). However, only a small amount of 3-OST-1 was present in the supernatant of *E. coli* TransB (DE3)/pET-20b-3-OST-I or *E. coli* BL21 (DE3)/pET-28a-3-OST-1 (Lane 3 and 7). Most of the 3-OST-1was present in an inactive form in inclusion bodies (Lane 4 and 8). The expected molecular mass of the fusion protein was 37.7 kDa via DNAMAN software analysis. After analysis via UN-SCAN-IT gel 6.1 software, the molecular weight of target band protein on SDS-PAGE was 37.8 kDa, suggesting the target protein was3-OST-1.

Renaturation was necessary to refold the target protein to obtain the active 3-OST-1. The renaturation process included denaturation, purification, and dialysis. The protein was successfully refolded during dialysis (Fig. 3, Lane 5). The three-dimensional structure of 3-OST-1 and distribution of hydrophobic amino acid residues was analyzed to reveal the structure of protein and mechanism of inclusion bodies formation, according to previously described methods [23]. The results (Fig. 4) showed that there are a large number of hydrophobic residues on the surface of the protein (Fig. 4B) that may result in the difficulty increasing for correct folding into the soluble protein.

In the refolding process, different initial concentrations of inclusion bodies resulted in varying degrees of precipitation by affecting its refolding rate (Fig. 5A). As the initial protein concentration increased, the refolding rate decreased. However, to balance the refolding efficiency, an initial inclusion body concentration of 0.08 mg/mL was selected in subsequent experiments. Different concentrations of glycerol [24] and polyethylene glycol [25] were added to reduce the precipitation and aggregation of proteins to further improve the refolding rate. The results are shown in Fig. 5B and C.

The enzyme activity of refolded HS3-OST-1 was detected by PAPS regeneration system. We found that the refolding conditions showed no significant effect on enzyme activity. After purification by Ni column, the protein concentration was 75.3 μg/mL, the enzyme activity was 0.04 U/mL with a specific enzyme activity of 0.53 U/mg.

3.3. Increased 3-OST-1 soluble expression by E. coli BL21 (DE3)/pET-28a-3-OST- 1 + pGro7

The recombinant strain *E. coli* TransB (DE3)/pET-20b-3-OST-1 showed that there was no significantly increase of 3-OST-1 expression level when compared to *E. coli* BL21 (DE3)/pET-28a-3-OST-1. Therefore, the co-expression of recombinant plasmid pET-28a-3-OST-1 with the chaperone expression system (pGro7) was constructed. The 3-OST-1 soluble expression was significantly improved by the co-expression by recombinant strain *E. coli* BL21 (DE3)/pET-28a-3-OST-1 + pGro7 (Fig. 6, Lane 8 and Lane 10), with enzyme activity reaching 0.06 U/mL and the specific activity reaching 0.87 U/mg (Table 1). The effect of temperature, arabinose concentration, and IPTG concentration on the 3-OST-1 expression in *E. coli* BL21 (DE3)/pET-28a-3-OST-1 + pGro7 were evaluated (Fig. 7).

3.4. 3-O-sulfo modification of NSNAH by 3-OST-1

The 3-*O*-sulfo modification of NSNAH was performed to verify the function of the 3-OST-1 protein which is expressed by *E. coli* BL21 (DE3)/pET-28a-3-OST-1 + pGro7. In this experiment, 20 mg NSNAH was used. After dialysis, concentration and freeze-drying, a total of 17.8 mg NSNA3SHp was obtained corresponding to a recovery rate of 89.1%. The ^{1}H -NMR of NSNA3SHp and NSNAH are shown in Fig. 8. The results show that GlcNS3S H1 peak was observed at 5.52 ppm and GlcNS3S H3 peak was observed at 3.82 ppm, indicating that NSNA3SHp had been successfully prepared.

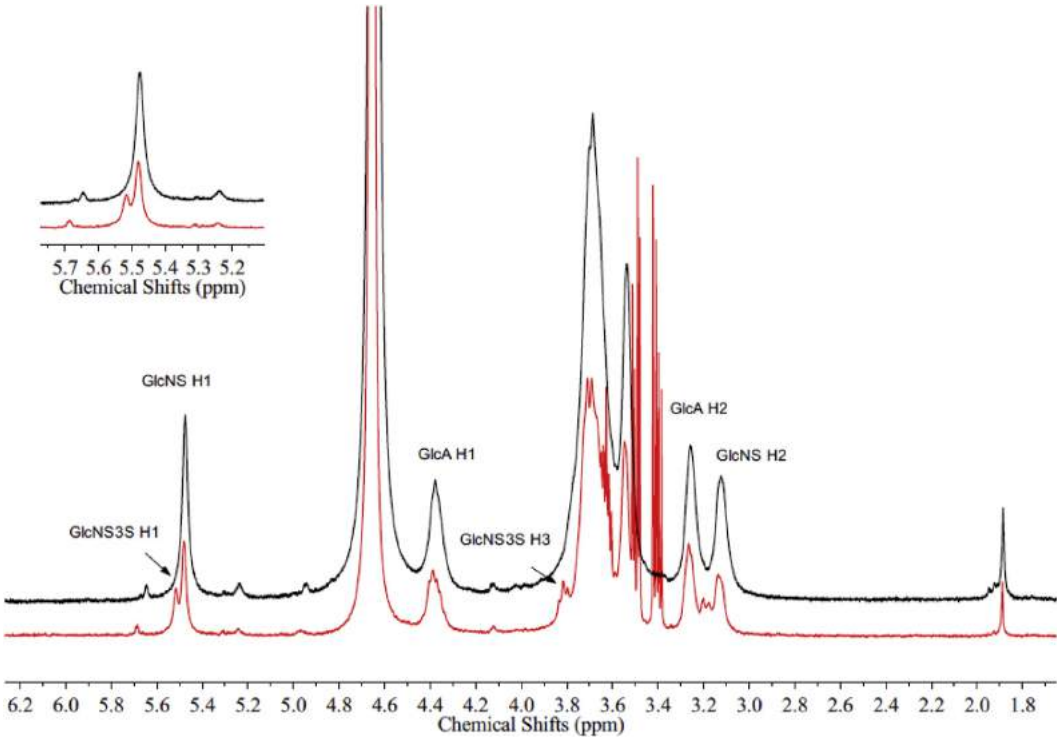

Fig. 8. ^{1}H NMR spectra comparison of the NSNAH (blank) and NSNA3SHp (red). (For interpretation of the references to colour in this figure legend, the reader is referred to the Web version of this article.)

4. Discussion

In the past decade, an increasing number of publications reported the heparin preparation strategy via chemical and enzymatic modification of heparosan from *E. coli* K5, including both high density fermentation and metabolic engineering modification of K5 strain and relative enzymes [26–33]. Both the biosynthesis of heparin and HS require a number of different enzymes but the final enzymes in the pathway, the 3-OSTs are critically involved in many of the critical biological functions of these GAGs [9]. For example, 3-OST-1 is critically important for the introduction of the AT binding site into HS and heparin. With the advent of bioengineered heparins and chemoenzymatically synthesized low molecular weight heparin and HS oligosaccharides, a new set of anticoagulant/antithrombotic drugs, are currently being explored [7,34]. Recently, 3-OST-1 has been used to convert low activity bovine intestinal heparin into a high activity heparin structurally similar to commercially used porcine intestinal heparin [35]. All of these studies rely on available highly active sources of recombinant 3-OST-1.

During past few decades, several laboratories reported the heterologous expression of 3-OST-1. A human sourced 3-OST-1 was expressed in *E. coli* by codon optimization as soluble 3-OST-1 [36]. The expression of only the catalytic domain (G48 to H311) of 3-OST-1 gene from mice was reported in *E. coli*, because it is not only catalytically effective region but also more hydrophilic region than the whole enzyme [23]. *Bacillus subtilis* and *Bacillus megaterium* were used a host cells to express the 3-OST-1 gene from mice to reduce the endotoxin content [22]. The resulting recombinant protein contained 10^{4}-10^{5} lower endotoxin levels than those obtained from *E. coli* strains. However, most 3-OST-1 expressed by *Bacillus subtilis* was found in inclusion bodies and the enzyme activity (0.3 U/mg) and yield of the soluble portion was low.

In summary, in most previous reports, the gene of 3-OST-1 was from mice and the soluble yield is not high. Additionally, it has been reported that the activity of 3-OST-1 is different in various tissues of mice, among which the brain showed the highest activity as 0.07 U/μL, while the lung and blood showed activity as 0.03 U/μL [37]. This finding suggests that 3-OST-1 may play an important role in the brain [17,38]. The large-scale application of bioengineered heparin production also requires the examination of various sources 3-OST-1 genes for cloning and enhanced soluble heterologous expression in hosts such as *E. coli*.

The present study has succeeded in the expression of 3-OST-1 gene, which was cloned from the brain of Wistar rats. The gene homology reached 99% and there were 5 different bases on comparison with the 3-OST-1 gene of *Rattus norvegicus* reported in NCBI. However, it was found that the expression level of this gene in *E. coli* was also very low. After codon optimization, the target protein was expressed in large amounts, but it was mostly in the form of inclusion bodies. Refolding conditions were optimized to obtain the active soluble protein. At protein concentrations in inclusion bodies of 0.08 mg/mL the addition of 5 g/L polyethylene glycol resulted in refolding percentages reaching 54.9%. The activity of the refolded protein reached 0.04 U/mL and the specific activity was 0.55 U/mg. Further increased 3-OST-1 soluble expression was achieved by *E. coli* BL21 (DE3)/pET-28a-3-OST-1 + pGro7, achieving enzyme activities 0.06 U/mL with specific activities of 0.87 U/mg. In addition, the substrates before and after modification by 3-OST-1 were analyzed by ^{1}H NMR showed that the 3-OST-1 modified NSNAH to afford NSNA3SHp.

In conclusion, 3-OST-1 from rat brain tissue could be expressed in *E coli*. The soluble target protein catalyzed the sulfation of NSNAH to obtain NSNA3SHp. The soluble expression level of active enzyme while be improved, still requires further work.

Compliance with ethical standards

The authors declare that they comply with ethical standards.

Conflicts of interest

The authors declare that they have no conflict of interest.

Ethical approval

All experiments were approved by the Research Committee of Zhejiang University of Technology, and the rats were carried out ethically and humanely.

Acknowledgments

This study was financially supported by the Natural Science Foundation of China (Grant No. 21076195, 41506165), the Science and Technology Department of Zhejiang Province (Grant No. 2011C24007), the Specialized Research Fund for the Doctoral Program of Higher Education (Grant No. 20113317110002), and the Open Research Fund of Zhejiang Province Top Key Discipline of Biological Engineering (2015).

Appendix A. Supplementary data

Supplementary data related to this article can be found at http://dx.doi.org/10.1016/j.pep.2018.06.007.

References

[1] C.M. Alexander, F. Reichsman, M.T. Hinkes, J. Lincecum, K.A. Becker, S. Cumberledge, M. Bernfield, Syndecan-1 is required for Wnt-1-induced mammary tumorigenesis in mice, Nat. Genet. 25 (2000) 329–332.
[2] M. Bernfield, M. Götte, P.W. Park, O. Reizes, M.L. Fitzgerald, A. John Lincecum, M. Zako, Functions of cell surface heparan sulfate proteoglycans, Annu. Rev. Biochem. 68 (1999) 729–777.
[3] J. Liu, S.C. Thorp, Cell surface heparan sulfate and its roles in assisting viral infections, ChemInform 33 (2010) no-no.
[4] R. O, L. J, W. Z, G. O, H. L, K. M, A. R, H. MT, B. GS, R. H, B. M, Transgenic expression of syndecan-1 uncovers a physiological control of feeding behavior by syndecan-3, Cell 106 (2001) 105.
[5] R.D. Rosenberg, N.W. Shworak, J. Liu, J.J. Schwartz, L. Zhang, Heparan sulfate proteoglycans of the cardiovascular system. Specific structures emerge but how is synthesis regulated? J. Clin. Invest. 99 (1997) 2062–2070.
[6] S. Peterson, A. Frick, J. Liu, Design of biologically active heparan sulfate and heparin using an enzyme-based approach, Nat. Prod. Rep. 26 (2009) 610.
[7] Z. Wang, B. Yang, Z. Zhang, M. Ly, M. Takieddin, S. Mousa, J. Liu, J.S. Dordick, R.J. Linhardt, Control of the heparosan N-deacetylation leads to an improved bioengineered heparin, Appl. Microbiol. Biotechnol. 91 (2011) 91–99.
[8] H.R. Pourianfar, C.L. Poh, J. Fecondo, L. Grollo, In vitro evaluation of the antiviral activity of heparan sulfate mimetic compounds against Enterovirus 71, Virus Res. 169 (2012) 22.
[9] B.E. Thacker, D. Xu, R. Lawrence, J.D. Esko, Heparan sulfate 3-O-sulfation: a rare modification in search of a function, Matrix Biol. 35 (2014) 60.
[10] D. Lembo, M. Donalisio, M. Rusnati, A. Bugatti, M. Cornaglia, P. Cappello, M. Giovarelli, P. Oreste, S. Landolfo, Sulfated K5 *Escherichia coli* polysaccharide derivatives as wide-range inhibitors of genital types of human papillomavirus, Antimicrob. Agents Chemother. 52 (2008) 1374–1381.
[11] E. Vicenzi, A. Gatti, S. Ghezzi, P. Oreste, G. Zoppetti, G. Poli, Broad spectrum inhibition of HIV-1 infection by sulfated K5 *Escherichia coli* polysaccharide derivatives, AIDS 17 (2003) 177–181.
[12] D. Shukla, J. Liu, P. Blaiklock, N.W. Shworak, X. Bai, J.D. Esko, G.H. Cohen, R.J. Eisenberg, R.D. Rosenberg, P.G. Spear, A novel role for 3-O-sulfated heparan sulfate in herpes simplex virus 1 entry, Cell 99 (1999) 13.
[13] J. Chen, M.B. Duncan, K. Carrick, R.M. Pope, J. Liu, Biosynthesis of 3-O-sulfated heparan sulfate: unique substrate specificity of heparan sulfate 3-*O*-sulfotransferase isoform 5, Glycobiology 13 (2003) 785.
[14] Sheng Ye, Yongde Luo, Weiqin Lu, Richard B. Jones, Robert J. Linhardt, Ishan Capila, Toshihiko Toida, Mikio Kan, Huguette Pelletier, Wallace L. McKeehan, Structural basis for interaction of FGF-1, FGF-2, and FGF-7 with different heparan sulfate motifs, Biochemistry 40 (2001) 14429.
[15] A.I. de Agostini, J.C. Dong, V.A.C. De, M.A. Ramus, I. Dentand-Quadri, S. Thalmann, P. Ventura, V. Ibecheole, F. Monge, A.M. Fischer, Human follicular fluid heparan sulfate contains abundant 3-O-sulfated chains with anticoagulant activity, J. Biol. Chem. 283 (2008) 28115–28124.
[16] N.W. Shworak, J. Liu, L.M.S. Fritze, J.J. Schwartz, L. Zhang, D. Logeart, R.D. Rosenberg, Molecular cloning and expression of mouse and human cDNAs encoding heparan sulfate d-glucosaminyl 3-*O*-sulfotransferase, J. Biol. Chem. 272 (1997) 28008–28019.
[17] T. Yabe, T. Hata, J. He, N. Maeda, Developmental and regional expression of heparan sulfate sulfotransferase genes in the mouse brain, Glycobiology 15 (2005) 982–993.
[18] D. Xu, A.F. Moon, D. Song, L.C. Pedersen, J. Liu, Engineering sulfotransferases to modify heparan sulfate, Nat. Chem. Biol. 4 (2008) 200.
[19] N.W. Shworak, J. Liu, L.M. Petros, L. Zhang, M. Kobayashi, N.G. Copeland, N.A. Jenkins, R.D. Rosenberg, Multiple isoforms of heparan sulfate D-glucosaminyl 3-*O*-sulfotransferase. Isolation, characterization, and expression of human cdnas and identification of distinct genomic loci, J. Biol. Chem. 274 (1999) 5170–5184.
[20] F. Dzierszinski, M. Mortuaire, M.F. Cesbron-Delauw, S. Tomavo, Targeted disruption of the glycosylphosphatidylinositol-anchored surface antigen SAG3 gene in *Toxoplasma gondii* decreases host cell adhesion and drastically reduces virulence in mice, Mol. Microbiol. 37 (2000) 574–582.
[21] M.D. Burkart, M. Izumi, E. Chapman, A. Chunhung Lin, C.H. Wong, Regeneration of PAPS for the enzymatic synthesis of sulfated oligosaccharides, J. Org. Chem. 65 (2000) 5565.
[22] W. Wang, J.A. Englaender, P. Xu, K.K. Mehta, J. Suwan, J.S. Dordick, F. Zhang, Q. Yuan, R.J. Linhardt, M. Koffas, Expression of low endotoxin 3-*O*-sulfotransferase in Bacillus subtilis and Bacillus megaterium, Appl. Biochem. Biotechnol. 171 (2013) 954–962.
[23] S.C. Edavettal, K.A. Lee, M. Negishi, R.J. Linhardt, J. Liu, L.C. Pedersen, Crystal structure and mutational analysis of heparan sulfate 3-*O*-sulfotransferase isoform 1, J. Biol. Chem. 279 (2004) 25789.
[24] Y. Maeda, H. Yamada, T. Ueda, T. Imoto, Effect of additives on the renaturation of reduced lysozyme in the presence of 4 M urea, Protein Eng. 9 (1996) 461.
[25] Y.J. Chen, L.W. Huang, H.C. Chiu, S.C. Lin, Temperature-responsive polymer-assisted protein refolding, Enzym. Microb. Technol. 32 (2003) 120–130.
[26] Z.Y. Wang, M. Ly, F. Zhang, W. Zhong, A. Suen, J.S. Dordick, R.J. Linhardt, *E. coli* K5 fermentation and the preparation of heparosan, Biotechnol. Bioeng. 107 (2010) 964–973.
[27] M. Ly, Z.Y. Wang, T.N. Laremore, F.M. Zhang, W.H. Zhong, D. Pu, D.V. Zagorevski, J. Dordick, R.J. Linhardt, Analysis of *E. coli* K5 capsular polysaccharide heparosan, Anal. Bioanal. Chem. 399 (2011) 737–745.
[28] H. Huang, Y. Zhao, S. Lv, W. Zhong, F. Zhang, R.J. Linhardt, Quantitation of heparosan with heparin lyase III and spectrophotometry, Anal. Biochem. 447 (2014) 46–48.
[29] H. Huang, S. Lv, L. Zhao, Z. Yan, W. Zhong, F. Zhang, Capsule treatment by soluble expressed recombinant heparinase II enhance the foreign gene transformation to *Escherichia coli* K5, J. Pure Appl. Microbiol. 7 (2013) 3009–3015.
[30] H. Huang, X. Li, N. Li, W. Zhong, Effect of enviromental stresses on heparosan biosynthesis by *Escherichia coli K5*, J. Pure Appl. Microbiol. 7 (2013) 3025–3029.
[31] J. Zhang, M. Suflita, G. Li, W. Zhong, L. Li, J.S. Dordick, R.J. Linhardt, F. Zhang, High cell density cultivation of recombinant *Escherichia coli* strains expressing 2-*O*-sulfotransferase and C5-Epimerase for the production of bioengineered heparin, Appl. Biochem. Biotechnol. 175 (2015) 2986–2995.
[32] G. Su, L. Li, H. Hang, W. Zhong, P. Yu, F. Zhang, R.J. Linhardt, Production of a low molecular weight heparin production using recombinant glycuronidase, Carbohydr. Polym. 134 (2015) 151–157.
[33] H. Huang, X. Liu, S. Lv, W. Zhong, F. Zhang, R.J. Linhardt, Recombinant *Escherichia coli* K5 strain with the deletion of waaR gene decreases the molecular weight of the heparosan capsular polysaccharide, Appl. Microbiol. Biotechnol. 100 (2016) 7877–7885.
[34] Y. Xu, K. Chandarajoti, X. Zhang, V. Pagadala, W. Dou, D.M. Hoppensteadt, E.M. Sparkenbaugh, B. Cooley, S. Daily, N.S. Key, Synthetic oligosaccharides can replace animal-sourced low-molecular weight heparins, Sci. Transl. Med. 9 (2017) 406.
[35] L. Fu, K. Li, D. Mori, M. Hirakane, L. Lin, N. Grover, P. Datta, Y. Yu, J. Zhao, F. Zhang, Enzymatic generation of highly anticoagulant bovine intestinal heparin, J. Med. Chem. 60 (2017) 8673–8679.
[36] J.R. Myette, Z. Shriver, J. Liu, G. Venkataraman, R. Rosenberg, R. Sasisekharan, Expression in Escherichia coli, purification and kinetic characterization of human heparan sulfate 3-*O*-sulfotransferase-1, Biochem. Biophys. Res. Commun. 290 (2002) 1206–1213.
[37] S. Hajmohammadi, K. Enjyoji, M. Princivalle, P. Christi, M. Lech, D. Beeler, H. Rayburn, J.J. Schwartz, S. Barzegar, A.I. de Agostini, Normal levels of anticoagulant heparan sulfate are not essential for normal hemostasis, J. Clin. Invest. 111 (2003) 989–999.
[38] H. Mochizuki, K. Yoshida, Y. Shibata, K. Kimata, Tetrasulfated disaccharide unit in heparan sulfate: enzymatic formation and tissue distribution, J. Biol. Chem. 283 (2008) 31237–31245.